AD-A282 233

ATION PAGE

[form instructions text, illegible]

	2. REPORT DATE	3. REPORT TYPE AND DATES COVERED
(Leave blank)	July 13, 1994	Technical Report #4

4. TITLE AND SUBTITLE	5. FUNDING NUMBERS
Electronic Energy Transfer in New Polymer Nanocomposite Assemblies	N00014-94-1-0540
6. AUTHOR(S)	Kenneth J. Wynne
C.-J. Yang and S.A Jenekhe	R & T Code: 3132111

7. PERFORMING ORGANIZATION NAME(S) AND ADDRESS(ES)	8. PERFORMING ORGANIZATION REPORT NUMBER
Department of Chemical Engineering University of Rochester 206 Gavett Hall ROchester, NY 14627-0166	#4

DTIC
ELECTE
JUL 27 1994
S B

9. SPONSORING/MONITORING AGENCY NAME(S) AND ADDRESS(ES)	10. SPONSORING/MONITORING AGENCY REPORT NUMBER
Office of Naval Research 800 North Quincy Street Arlington, VA 22217-5000	

94-23455

12a. DISTRIBUTION/AVAILABILITY STATEMENT	12b. DISTRIBUTION CODE
Reproduction in whole or in part is permitted for any purpose of the United States Government. This document has been approved for public release and sale; its distribution is unlimited.	

13. ABSTRACT (Maximum 200 words)

New light-harvesting thin film supramolecular assemblies, consisting of rod-coil polymer nanocomposites as the light-absorbing energy donors and a randomly dispersed conjugated rigid-rod polymer as the energy acceptor, have been prepared and shown to exhibit efficiency for singlet electronic energy transfer as high as 93%. The film thickness dependence of energy-transfer efficiency allowed us to determine the contributions of Förster and radiative mechanisms to energy transfer in the polymer nanocomposite assemblies. The Förster energy transfer efficiency was found to increase with increasing acceptor concentration, reaching an asymptotic maximum of 48% at ~3%. On the other hand, radiative transfer diminished to an insignificant contribution at low acceptor concentration (< 1 mol%). The Förster energy transfer efficiency varied significantly with the length of the flexible coil segment which regulates the supramolecular structure of the photoactive nanocomposite energy donor. The average intersite distance between donor and acceptor chromophores was measured spectroscopically to be in the range of 10 to 25 Å with corresponding Förster radii of 19-23 Å in the three series of supramolecular donor/acceptor assemblies investigated, depending on the acceptor concentration. The present results on novel light-harvesting polymer nanocomposite assemblies represent the successful supramolecular regulation of efficient electronic energy transfer in thin films and hence are promising for exploring optoelectronic applications.

14. SUBJECT TERMS			15. NUMBER OF PAGES
Polymer nanocomposites, electronic energy transfer; light-harvesting assemblies; supramolecular regulation; conjugated polymers.			36
			16. PRICE CODE

17. SECURITY CLASSIFICATION OF REPORT	18. SECURITY CLASSIFICATION OF THIS PAGE	19. SECURITY CLASSIFICATION OF ABSTRACT	20. LIMITATION OF ABSTRACT
Unclassified	Unclassified	Unclassified	Unlimited

94 7 25 109

DTIC QUALITY INSPECTED 1

OFFICE OF NAVAL RESEARCH

GRANT N00014-94-1-0540

R&T Code 3132111

Kenneth J. Wynne

Technical Report No. 4

Electronic Energy Transfer in New Polymer Nanocomposite Assemblies

by

Chen-Jen Yang and Samson A. Jenekhe

Prepared for Publication

in

Supramolecular Science

University of Rochester
Department of Chemical Engineering
Rochester, NY

July 13, 1994

TECHNICAL REPORT DISTRIBUTION LIST - GENERAL

Office of Naval Research (1)*
Chemistry and Physics Division
Ballston Tower 1, Room 503
800 North Quincy Street
Arlington, Virginia 22217-5660

Dr. Richard W. Drisko (1)
Naval Civil Engineering
 Laboratory
Code L52
Port Hueneme, CA 93043

Defense Technical Information
 Center (2)
Building 5, Cameron Station
Alexandria, VA 22314

Dr. Harold H. Singerman (1)
Naval Surface Warfare Center
 Carderock Division Detachment
Annapolis, MD 21402-1198

Dr. James S. Murday (1)
Chemistry Division, Code 6100
Naval Research Laboratory
Washington, D.C. 20375-5000

Dr. Eugene C. Fischer (1)
Code 2840
Naval Surface Warfare Center
 Carderock Division Detachment
Annapolis, MD 21402-1198

Dr. Kelvin Higa (1)
Chemistry Division, Code 385
Naval Air Weapons Center
 Weapons Division
China Lake, CA 93555-6001

Dr. Peter Seligman (1)
Naval Command, Control and
 Ocean Surveillance Center
RDT&E Division
San Diego, CA 92152-5000

* Number of copies to forward

Electronic Energy Transfer In New Polymer Nanocomposite Assemblies

Chen-Jen Yang and Samson A. Jenekhe*

Department of Chemical Engineering
and
Center for Photoinduced Charge Transfer
University of Rochester, Rochester, New York 14627-0166

Abstract

New light-harvesting thin film supramolecular assemblies, consisting of rod-coil polymer nanocomposites as the light-absorbing energy donors and a randomly dispersed conjugated rigid-rod polymer as the energy acceptor, have been prepared and shown to exhibit efficiency for singlet electronic energy transfer as high as 93 %. The film thickness dependence of energy-transfer efficiency allowed us to determine the contributions of Förster and radiative mechanisms to energy transfer in the polymer nanocomposite assemblies. The Förster energy transfer efficiency was found to increase with increasing acceptor concentration, reaching an asymptotic maximum of 48% at ~3 mol%. On the other hand, radiative transfer diminished to an insignificant contribution at low acceptor concentration (< 1 mol%). The Förster energy transfer efficiency varied significantly with the length of the flexible coil segment which regulates the supramolecular structure of the photoactive nanocomposite energy donor. The average intersite distance between donor and acceptor chromophores was measured spectroscopically to be in the range of 10—25 Å with corresponding Förster radii of 19—23 Å in the three series of supramolecular donor/acceptor assemblies investigated, depending on the acceptor concentration. The present results on novel light-harvesting polymer nanocomposite assemblies represent the successful supramolecular regulation of efficient electronic energy transfer in thin films and hence are promising for exploring optoelectronic applications.

* To whom correspondence should be addressed.

Introduction

Considerable interest has recently been directed to electronic energy transfer in various assemblies of organic molecules and polymers as simple models of biological photosynthesis processes and also owing to their potential for optoelectronic applications.[1-5] The photophysical and photochemical processes involved in these systems are mainly photosensitization, electronic energy migration and transfer through the assemblies to the energy trap, and subsequent charge generation and charge separation, or chemical reactions in the trap molecules.[1-4] Efficient electronic energy transfer (EET) from the energy donors to the energy acceptors in these systems is critical for viable artificial photosynthesis, photovoltaic devices, or other optoelectronic applications.

Many studies on the electronic energy transfer through pendant chromophores on flexible chain polymers have been reported.[6-13] It has been found that EET efficiency depends strongly on the polymer chain conformation in solution.[8-10] Several other factors such as solvent, PH value, and polymer molecular structure, were shown to be critical for efficient energy transfer from donor chromophores, pendant along the polymer backbone, to acceptor chromophores that are located at chain ends.[8-10] Much progress has been made towards understanding of the photophysics of EET in organic materials by using flexible-polymer/pendant-chromophore model systems. High EET efficiencies (60—100 % in solution, 43 % in solid matrices) have been obtained by optimization of polymer chain conformation and the judicious choice of donor-acceptor pairs.[3,6-13] However, excimer formation within the donor chromophores in this system may lead to a limitation on the achievable energy-transfer efficiency.[3-5,8-10] Also, the flexible-chain/pendant-chromophore system is not amenable to photovoltaic effects due to the limited distance for charge separation and the resulting energy-wasting back electron transfer.[4,5] For this reason, applications of pendant-chromophore assemblies are mainly in photochemical reactions.[14-16] For example, Guillet and coworkers have reported a series of photocatalytic activity studies of polymer micelles that have efficient electronic energy transfer.[14-16]

Numerous studies have verified the Förster mechanism of EET between chromophores in solutions and solid polymer matrices.[8-13,17] According to the Förster equation for energy transfer

by dipole-dipole interaction, the energy-transfer rate is inversely proportional to the 6th power of the interchromophore distance, if extensive overlap of donor emission with acceptor absorption is achieved.[18] As a result of the close agreement between experimental data and Förster's theory, EET has been utilized as a spectroscopic ruler to determine intermolecular distances.[19-21] A related application is the use of fluorescence spectroscopy as a method for determining molecular-level miscibility of polymer blends.[22,23] Morawetz and coworkers have reported a series of such studies of polymer blends,[22] in which fluorescent chromophores were attached at polymer chain ends as energy donors and acceptors and the miscibility of the polymer blends was determined by measuring the relative intensities of the donor and acceptor emission.[22]

Unlike pendant-chromophore/flexible-chain polymer systems electronic energy transfer in conjugated polymers has not received much interest.[24,25] Energy migration between segments with different conjugation lengths of the same species has been reported.[24,25] The finding that the emission of conjugated polymers is dominated by the lowest-energy state has suggested that *electronic energy migration is facile in conjugated polymers.*[24,25] In a series of studies of the luminescence of conjugated polymers, it has been shown that by incorporating flexible-coil components into conjugated rigid-rod polymers, rod-coil copolymers in which the fluorescence quantum efficiency is enhanced by an order of magnitude are obtained.[26] Such rod-coil copolymers, termed *polymer nanocomposites*, are promising for optoelectronic applications owing to their photophysical properties which are regulated by supramolecular structure and morphology.[26]

In this paper, we explore solid state electronic energy transfer in novel supramolecular polymer assemblies comprised of photoactive rod-coil copolymers in which a conjugated rigid-rod polymer is randomly dispersed. The rod-coil copolymers or polymer nanocomposites are used as energy donor hosts. The energy acceptor in the present study is a dithienylvinylene-linked polyanthrazoline whose synthesis and characterization have previously been reported.[27] The molecular structures of the component materials are shown in Chart 1. The supramolecular donor/acceptor assemblies in which EET was investigated are homogeneous binary mixtures of the

3

component polymeric materials as illustrated in Chart 2. One particularly interesting feature of these energy donor/acceptor assemblies is that the energy trap being a conjugated polymer with extended π-electron delocalization would greatly reduce the probability of energy-wasting back electron transfer. Our objective in the present study is to investigate the use of the rod-coil polymer nanocomposites as the "antenna" in synthetic light-harvesting polymer assemblies containing a conjugated polymer acceptor. We also hoped to thereby explore the effects of supramolecular structure on the singlet EET efficiency in the new donor/acceptor nanocomposite assemblies.

Experimental Section

Materials. 1,4-Phenylenediamine (99%, Aldrich) was recrystallized from benzene. 1,10-Diaminodecane (97%, Aldrich) and 1,12-diaminododecane (98%, Aldrich) were purified by vacuum sublimation at 45 ^{0}C. 1,7-Diaminoheptane (98%, Aldrich) was used as received. Terephthaldehyde (98%, Aldrich) was purified by vacuum sublimation at 100 ^{0}C. The polymerization solvents, hexamethylenephosphoramide (HMPA) (99%, Aldrich) and 1-methyl-2-pyrrolidinone (NMP) (99+% anhydrous, Aldrich), and the water adsorbing reagent, lithium chloride (99+%, Aldrich), were used as received.

Preparation of Polymers. The rod-coil copolymers were synthesized by the solution condensation copolymerization of aromatic and aliphatic diamines with terephthaldehyde, similar to the synthesis of related homopolymers.[28]

PPI/PI-C7. 111.3 mg (1.029 mmol) 1,4-phenylenediamine and 201.1 mg (1.544 mmol) 1,7-diaminoheptane were reacted with 345.1 mg (2.573 mmol) terephthaldehyde in 6 ml 1:1 HMPA/NMP and 0.15 g LiCl under nitrogen purge at 80 ^{0}C. After 48 hr polymerization time, the copolymer was precipitated and washed repeated with water and methanol, and dried under vacuum to afford a light-yellow powder (410.0 mg, 73% yield). ^{1}H NMR of PPI/PI-C7 in $GaCl_3/CD_3NO_2$ (δ, ppm) : 1.60, 2.10, 4.25, 8.40, 8.75, 9.25, 9.85. Intrinsic viscosity [η] in $GaCl_3$/nitromethane at 30 ^{0}C : 1.38 dL/g.

PPI/PI-C10. 318.0 mg (2.94 mmol) 1,4-phenylenediamine and 760.1 mg (4.41 mmol)

4

1,10-diaminodecane were reacted with 986.1 mg (7.35 mmol) terephthaldehyde in 12 ml 1:1 HMPA/NMP containing 0.5 g LiCl at 80 °C. After 48 hr polymerization time, the polymer was purified to afford a light-yellow powder (1342.1 mg, 75 % yield). ^{1}H NMR of PPI/PI-C10 in GaCl$_3$/CD$_3$NO$_2$ (δ, ppm) : 1.40, 2.05, 4.25, 8.40, 8.65, 8.75, 9.25, 9.90. Intrinsic viscosity [η] in GaCl$_3$/nitromethane at 30 °C : 1.66 dL/g.

PPI/PI-C12. 87.4 mg (0.81 mmol) 1,4-phenylenediamine and 242.9 mg (1.21 mmol) 1,12-diaminododecane were reacted with 271.0 mg (2.02 mmol) terephthaldehyde in 8 ml 1:1 HMPA/NMP containing 0.15 g LiCl at 80 °C. After 48 hr polymerization time, the polymer was purified to afford a light-yellow powder (377.5 mg, 71 % yield). ^{1}H NMR of PPI/PI-C12 in GaCl$_3$/CD$_3$NO$_2$ (δ, ppm) : 1.40, 2.00, 4.20, 7.80, 8.35, 8.60, 9.25, 9.80. Intrinsic viscosity [η] in GaCl$_3$/nitromethane at 30 °C : 1.79 dL/g.

PBTVDA[27]. The synthesis and characterization of the bithienylene-linked poly-anthrazoline, PBTVDA, and other thiophene-linked polyquinolines and polyanthrazolines have previously been reported.[27]

Blend and Thin Film Preparation. Soluble Lewis or diarylphosphate complexes of the polymers in nitromethane or m-cresol, respectively, were prepared as described in our earlier studies.[28] However, to facilitate the spin coating of very thin films for fluorescence measurements, trifluoroacetic acid or formic acid was used in place of m-cresol as the solvent for the diarylphosphate complexes of the polymers. For the preparation of the diarylphosphate complexes of copolymers, a molar ratio (DPP:CH=N) of 0.5:1 was used in complexation. The concentration of the complexes in trifluoroacetic acid was varied in the range of 0.1—0.5 wt%, and the speed of spin coating was adjusted between 1800—3200 rpm to prepare uniform thin films. After drying overnight in a vacuum oven, thin films of the complexes were immersed in triethylamine/methanol to obtain thin films of pure copolymers. The resulting film thickness, measured by an alpha-step profilometer and absorbance of the optical absorption spectra, was varied in the range 20—100 nm. Prior to preparing thin films of the blends of the copolymers with the rigid-rod polymer PBTVDA, a stock solution of PBTVDA was prepared in advance by reacting the polymer with

DPP in 1:1 trifluoroacetic acid/formic acid. Solutions of the blends were prepared by mixing the copolymer, the stock solution of PBTVDA, and DPP in trifluoroacetic acid. Thin films of the blends were prepared and regenerated according to the same procedures as for the thin films of pure copolymers. The concentration of PBTVDA in the solid polymer blends, expressed in mol% based on polymer repeat unit, was determined by the amount of stock solution and the copolymer used in the preparation.

Fluorescence Spectra. Steady-state photoluminescence studies were done on a Spex Fluorolog-2 fluorometer equipped with a computer-driven DM3000F program. All fluorescence measurements were done at room temperature. The polymer films on glass slides were positioned such that the emission was detected at 22.5^0 from the incident beam. The relative fluororescence quantum efficiencies of the thin films of three rod-coil copolymers were determined from the integrated emission intensity of fluororescence spectra, corrected for absorbance at the excitation wavelength that was kept at ~0.1 for all three copolymer films. To estimate the absolute quantum efficiency, we used ~10^{-3} M 9,10-diphenylanthracene in poly(methyl methacrylate) as a standard (ϕ = 83 %).[31]

Results and Discussion

The three photoactive rod-coil copolymers (see Chart 1), PPI/PI-Cx (x = 7, 10, 12), were synthesized and their structures were characterized prior to preparing their blends with the conjugated rigid-rod polyanthrazoline, PBTVDA. The molecular structures and compositions of the copolymers were characterized by ^{1}H NMR spectra.[28] The composition of the conjugated rigid-rod segment in PPI/PI-C7, PPI/PI-C10, and PPI/PI-C12 was 36, 31, and 29 mol%, respectively. A typical NMR spectrum of the rod-coil copolymers is shown in Figure 1 for the PPI/PI-C7 case. The composition of PPI/PI-C7, that indicates a 36 mol%-PPI segments, was determined readi!y from the ratio of the integration of the methylene-proton resonance peaks at 1.60 and 2.10 ppm, to the imine-proton resonance peaks at 9.25 and 9.85 ppm. The compositions of the other rod-coil copolymers were similarly determined.

The main difference between the three rod-coil copolymers (Chart 1) is the length of the flexible coil segments which varies from 7 methylene groups in PPI/PI-C7 to 10 and 12 methylene groups in PPI/PI-C10 and PPI/PI-C12, respectively. This variation in the overall flexibility of the rod-coil chains of PPI/PI-Cx is expected to lead to a variation in the supramolecular structure and morphology of the three host donors and, upon blending with rodlike PBTVDA, a variation in the supramolecular structure of the donor/acceptor assemblies. Thus, although the concentration of the photoactive rodlike segments is approximately the same (29—36 mol% PPI) in the donor hosts PPI/PI-Cx, we expect a difference in the photophysical properties and electronic energy transfer due to variation in supramolecular structure.

Thin films of the copolymers and their blends with PBTVDA were prepared by spin coating the trifluoroacetic acid/formic acid solutions of their complexes with diphenyl phosphate (DPP).[27,28] Film thickness was varied by varying the concentration of solutions and the speed of spin coating and was kept at 100 nm or less so that the optical density (absorbance) of the thin films was below 0.3. In our EET experiments the film thickness was between 20 and 100 nm. Thin films of the spin coated polymer DPP complexes were dried at 60 °C in vacuum followed by the immersion in triethylamine/ethanol overnight for regeneration to afford thin films of the pure copolymers and blends. The decomplexation/regeneration process was facile as evidenced by the instant color change, for example, from the orange color of the complex of PPI/PI-Cx with DPP to the light yellow color of pure PPI/PI-Cx. In our previous studies, the reversibility of the conversion between complexes and pure polymers has been verified by thermal analysis and spectroscopic characterization methods.[27,28] For these particular rigid-rod/flexible-coil copolymers, the regenerated materials were also characterized and shown to be identical to the pristine polymers by thermogravimetric analysis (TGA), differential scanning calorimetry (DSC), and Fourier transform infrared (FTIR) spectroscopy.

Morphology and Stability of Supramolecular Assemblies

Molecular composites of polymers have been the subject of active research due to not only

the expected molecular-level reinforcement of mechanical properties[29] but also because of the recent discovery of improvement in optical and nonlinear optical properties.[30] The needed molecular-level dispersion of the rigid-rod and the flexible-coil polymers in such systems can be very difficult to achieve due to the entropically driven tendency toward demixing.[30] In a recent study of the morphology of rod/coil polymer blends prepared by complexation-mediated processing by differential scanning calorimetry (DSC), scanning electron microscopy (SEM) and x-ray diffraction, it was shown that molecular-level mixing in the solid rod/coil blends can be achieved by rapid evaporation of the solvent and thereby "freezing in" the molecular dispersion.[30] We have similarly investigated the morphology and stability of the donor/acceptor blends of PBTVDA with PPI/PI-Cx by DSC analysis.

Figure 2 shows the DSC thermograms of the pure PPI/PI-C12 (curve a), PBTVDA (curve b) and the blend consisting of 8.7 mol% PBTVDA in PPI/PI-C12 (curves c and d). The samples of the blend for DSC analysis were obtained from the solid films spin coated on glass slides by the complexation-decomplexation processes. The 8.7 mol%-PBTVDA blend is the highest acceptor concentration used in the energy-transfer studies. Up to the verge of thermal decomposition, neither PPI/PI-C12 nor PBTVDA show any phase transition as evidenced by their DSC thermograms in Figure 2. Interestingly, the 8.7 mol%-PBTVDA blend shows an endothermic transition at 250 ^{0}C that indicates an enthalpy of transition of 21.4 J/g (6.3 kJ/mol) in the first heating (Figure 2, curve c). However, no phase transition is observed in the second heating of the same sample of the blend (Figure 2, curve d). A reasonable explanation for the observed endothermic transition in the first DSC run of the blend is a thermally-induced phase separation of the otherwise single-phase mixture of PBTVDA and PPI/PI-C12. Following the phase separation, the blend retains the individual phase behaviors of pure components and therefore no phase transition is observed in the second heating. Similar DSC analyses on the as-prepared thin films of pure components and blends of PPI/PI-C7 and PPI/PI-C10 showed that a single-phase dispersion of the rigid-rod PBTVDA in the nanocomposites PPI/PI-Cx was also obtained at below ~200—250 ^{0}C. Therefore, subsequent studies of the photophysical properties of the PBTVDA—PPI/PI-Cx

8

blends reflect those of a single-phase, rather than phase-separated, mixtures of PBTVDA and PPI/PI-Cx.

Photophysical Properties of Supramolecular Assemblies

The optical absorption and fluorescence spectra of the component energy donors and acceptors are first discussed prior to the supramolecular assemblies of the components. Figure 3 shows the optical absorption and fluorescence spectra of PPI/PI-C12 and PBTVDA thin films. The rod-coil copolymer PPI/PI-C12 exhibits a λ_{max} at 370 nm in the absorption and two peaks with λ_{max} at 530 and 560 nm in the emission spectra. The conjugated rigid-rod polymer, PBTVDA, absorbs and emits at longer wavelengths, with λ_{max} at 532 nm in the absorption and 650 nm in the emission, respectively. The corresponding excitation wavelengths for the emission spectra were 420 nm and 530 nm for PPI/PI-C12 and PBTVDA, respectively. Relative to the absorption spectra, a significant red shift (>100 nm, 1.0 eV) is observed in the emission of both PPI/PI-C12 and PBTVDA. This large apparent Stokes shift has been attributed to energy migration among segments of different conjugation lengths in conjugated polymers.[24,25] However, an alternative interpretation in terms of excimer formation has been proposed.[26] The data for the absorption and emission spectra of the component materials are listed in Table 1.

The fluorescence spectra of PPI/PI-C7, PPI/PI-C10, PPI/PI-C12, and PBTVDA are shown in Figure 4 for comparison. The emission spectra of the three rod-coil copolymers, PPI/PI-C7, PPI/PI-C10 and PPI/PI-C12, are very similar regardless of the differences in the flexible-coil lengths in their structures. However, a reduced intensity is observed in the emission spectra of PPI/PI-C7 and PPI/PI-C10 relative to PPI/PI-C12. Using ~10^{-3} M 9,10-diphenylanthracene in poly(methyl methacrylate) as a fluorescence standard (ϕ = 83 %),[31] the fluorescence quantum efficiency of PPI/PI-C7, PPI/PI-C10, PPI/PI-C12, and PBTVDA were calculated and are listed in Table 1. The quantum yield values are in the range of 0.31—0.74 %. Relative to the host with the shortest length of flexible coil segment (PPI/PI-C7), the fluorescence quantum yields of PPI/PI-C10 and PPI/PI-C12 are enhanced by factors of 2.1 and 2.4, respectively. The variation in

9

fluorescence quantum yield of the polymer nanocomposites PPI/PI-Cx with length of the coil segments can be explained in terms of the varying supramolecular structure which in turn regulates the degree of excimer formation and self-quenching.[26]

An interesting observation in the absorption and emission spectra in Figure 3 is the overlap of the emission of PPI/PI-C12 (donor chromophore) with the absorption of PBTVDA (acceptor chromophore), a prerequisite for efficient Förster-type energy transfer from donors to acceptors. The Förster radius can be determined by the overlapped integral of the emission and absorption spectra :

$$R_{DA} = \left(\frac{9\kappa^2 \phi_D}{128\pi^5 n^4 N'} \int \frac{f_D(v)\alpha_A(v)}{v^4} \, dv \right)^{\frac{1}{6}} \tag{1}$$

in which R_{DA} is the Förster radius for energy transfer from donor to acceptor, κ is the orientation factor usually taken as 2/3, ϕ_D is the quantum efficiency for donor emission, n is the refractive index, N' is the number density of acceptors, $f_D(v)$ is the normalized donor emission intensity as a function of frequency v, and α_A is the absorption coefficient of the acceptor.[18,32] From the measured absorption and emission spectra, the Förster radius R_{DA} for energy transfer in the polymer nanocomposite assemblies was determined to be 19.1, 21.0, and 22.5 Å for PPI/PI-C7, PPI/PI-C10, and PPI/PI-C12, respectively, as donors and PBTVDA as acceptor. Similarly, the Förster radii for energy migration between donor chromophores (R_{DD}) and between acceptor chromophores (R_{AA}) were also calculated and are listed in Table 2. The Förster radius R_{DD} varies from 9 to 11.7 Å for EET among the donor chromophores whereas the corresponding radius R_{AA} for EET among acceptor chromophores is 16.3 Å.

Figure 5 shows the emission spectra of a 3.4 mol% PBTVDA—PPI/PI-C12 blend when excited at a wavelength of 420 nm (curve a) or 530 nm (curve b). The donor/acceptor assembly emits light with peaks at 530 and 650 nm when excited at 420 nm, but only the 650-nm emission is observed when excited at 530 nm, the absorption maximum of the acceptor. The 650-nm emission

can be readily assigned to the emission of the acceptor PBTVDA since it exhibits the same features as the pure acceptor emission. Furthermore, the intensity of the 650-nm emission when the acceptor is directly excited at 530 nm is only a factor of 0.63 compared to that when the donor is excited at 420 nm. These results clearly suggest that the occurence of EET from the donor PPI/PI-C12 to the energy acceptor PBTVDA which exhibits a much smaller excitation energy relative to the donor (Table 1). However, given the broad absorption of the acceptor PBTVDA shown in Figure 3, it is possible that the 650-nm emission originates partly from direct acceptor excitation even at 420 nm. We have separately measured the emission spectra of the pure PBTVDA film by exciting at 420 nm or 530 nm and the results showed that the emission intensity by 420-nm excitation is only a factor of 1/7 of that due to 530-nm excitation of the same pure PBTVDA film. This observation indicates that only a small portion (~14 %) of the 650-nm emission of the donor/acceptor assembly is derived from a direct excitation of the acceptor. Thus, EET is the predominant (~86 %) origin of the emission of the donor/accepor assembly. Even so, the 420-nm direct excitation of the acceptor is still accounted for in subsequent analysis of EET efficiency in the donor/acceptor supramolecular assemblies. Measurement of the fluorescence spectra of other PBTVDA—PPI/PI-Cx assemblies showed similar features that indicate efficient EET in the polymer nanocomposite assemblies.

The fluorescence spectra of thin films (~100 nm) of PPI/PI-C12 based donor/acceptor assemblies with varying acceptor concentration are shown in Figure 6 for excitation at 420 nm. These spectra were normalized relative to the 530-nm donor emission intensity. The increase of acceptor emission intensity with increasing acceptor concentration is observed. These results show a strong dependence of EET on acceptor concentration. Although it can be expected that the Förster energy transfer through dipole-dipole interaction between donor and acceptor chromophores plays an important role in these polymer nanocomposite assemblies, the possibility of radiative transfer (trivial mechanism) contribution cannot be ruled out. This is because of the extensive overlap of donor emission with acceptor absorption (Figure 3) which could facilitate acceptor reabsorption of light emitted by the donor. To investigate the separate contributions of

11

radiative and nonradiative (Förster) energy transfer, the fluorescence spectra of films of the donor/acceptor blends with varying thickness were measured to show the film thickness dependence of EET in the materials. Figure 7 shows the flourescence spectra of 2.9 mol% PBTVDA in PPI/PI-C12 with varying film thickness from 29 to 96 nm. The fluorescence spectra in Figure 7 were normalized with the donor emission intensity at 530 nm. Clearly, the acceptor emission intensifies with increasing film thickness, suggesting that the contribution of radiative energy transfer must be accounted for in the analysis of EET efficiency.

EET Efficiency in Supramolecular Assemblies

From the measured fluorescence spectra that show both the emission of the donor and the acceptor, the efficiency χ for EET can be determined from the integrated emission intensity of the acceptor and the donor :[1]

$$\chi = \frac{\dfrac{I_A}{\phi_A}}{\dfrac{I_A}{\phi_A} + \dfrac{I_D}{\phi_D}} = \frac{\phi_D}{\phi_D + \phi_A \cdot \dfrac{I_D}{I_A}} \qquad (2)$$

where I_A and I_D are the integrated fluorescence intensities of the acceptor and donor, respectively. ϕ_A and ϕ_D are the fluorescence quantum efficiencies of the acceptor and donor, respectively. The acceptor emission intensity was corrected for the 420-nm direct excitation of the acceptor as stated previously. A spectra deconvolution computation method based on the Gaussian-lineshape function was used to resolve the partially overlapped emission of the donor and acceptor. In calculating the EET efficiency χ according to equation (2), it is assumed that the fluorescence quantum yields of the donor and acceptor (ϕ_D, ϕ_A) in the donor/acceptor blends remain the same as those for the pure individual components.[1,3] The energy-transfer efficiency χ as a function of film thickness is shown in Figure 8 for two acceptor concentrations, 2.9 mol% (a) and 0.6 mol%-PBTVDA (b) blends with PPI/PI-C12. Clearly, a strong dependence of the EET efficiency on film

12

thickness is observed in the case of the 2.9 mol% blend. The efficiency varies from 52 % to 64 % for the 2.9 mol% blend when the film thickness varied from 29 nm to 96 nm. In fact, a linear relationship between χ and film thickness d is obtained for the data shown in Figure 8. However, it was found that the thickness dependence of χ lessened with decreasing acceptor concentration until 0.6 mol% PBTVDA in which the energy-transfer efficiency is a constant independent of film thickness. The χ values of the 0.6 mol%— PBTVDA blend shown in Figure 8 indicate a constant efficiency of 30 % throughout the 22—87-nm film thickness range. The elimination of film thickness dependence of χ at low acceptor concentration suggests that the origin of χ's scaling with film thickness is due to the contribution of radiative component to the energy transfer in thicker films. It is therefore reasonable to extrapolate $\chi(d)$ to vanishing thickness (d=0) to obtain the Förster energy transfer efficiency. This is the case where reabsorption of donor emission by the acceptor is completely eliminated and consequently energy transfer is due entirely to the Förster mechanism (nonradiative). This procedure allowed us to determine the separate Förster mechanism and radiative contribution to EET efficiency of the nanocomposite donor/acceptor assemblies. The film thickness dependent EET efficiency $\chi(d)$ of all the donor/acceptor polymer blends (PPI/PI-Cx with varying concentrations of PBTVDA) was measured and from it the Förster energy transfer efficiency was obtained.

The acceptor concentration dependence of the overall EET efficiency χ (d~100 nm) and the Förster EET efficiency χ (d=0) of the three series of polymer nanocomposite assemblies are shown in Figure 9 and Table 3. Both the overall efficiency (Figure 9, open symbol) and the Förster component of the EET efficiency (Figure 9, filled symbol) increase with acceptor concentration until saturation. The highest overall EET efficiency is 93 % at ~8 mol% PBTVDA in PPI/PI-C12. The corresponding Förster EET efficiency is 48 %.

The most striking feature of the EET results in Figure 9 and Table 3 is the large effect of the donor host (PPI/PI-Cx, x= 7, 10, 12) on the efficiency. The maximum Förster energy transfer efficiency drops dramatically from 48 % and 42 % in PPI/PI-C12 and PPI/PI-C10, respectively, to 14.4 % in PPI/PI-C7. This means that there is a factor of 3.3 in the Förster EET efficiency in

13

going from the 7-methylene to the 12-methylene linked donor host. Another interesting observation from Figure 9 is the progressive shift of the critical acceptor concentration at which the nonradiative EET efficiency reaches asymptotic maximum, being about 1.0, 2.5, and 3.0 mol% PBTVDA for —C7, —C10, and —C12 rod-coil copolymers, respectively.

The present results clearly demonstrate that a molecularly well-defined approac! variation of coil segment length in the photoactive rod-coil copolymer hasts (Chart 1), can be to regulate EET efficiency in thin film polymer nanocomposite assemblies. The observed variation of EET efficiency with polymer chain flexibility can be explained by the effects of the rod-coil chain structure on chain packing in the solid state (i.e. supramolecular structure and morphology) which in turn has profound effects on the photophysical processes in the materials.[26] As previously discussed, the fluorescence quantum yield of the light-absorbing hast copolymers PPI/PI-Cx was enhanced by up to a factor of 2.4 in going from x=7 to 12 due to the progressive reduction of the degree of excimer formation and self-quenching with length of the flexible coil. However, the observed differences in the EET efficiency of the supramolecular donor/acceptor assemblies cannot be accounted for completely by the differences in the fluorescence quantum yields of the donor nanocomposites. We suggest as another factor, effects of the flexible coil length on the supramolecular structure of the donor/acceptor assemblies. The photophysical process involved would be supression or reduction of exciplex formation between excited donor molecules and ground state acceptor molecules that may lead to nonradiative decay of the electronic energy.

Another factor that explains the observed variation of EET efficiency with rod-coil chain flexibility is energy migration among donor molecules as depicted schematically in Chart 3. Sufficiently long flexible coil segments while reducing excimer formation also allow efficient energy migration among donors and this would facilitate sensitization of acceptor molecules by not only the nearest neighbor donor molecules but also distant donors. Thus, due to the multiple sensitization of the acceptor, the supramolecular donor/acceptor assembly exhibits intense acceptor emission even though at low acceptor concentration. It has been reported that the observed efficient

energy transfer of the pendant-chromophore system in glassy solid polymer matrices is due to facile energy migration between donors.[8] For efficient energy migration among donors, donors need to be brought to close vicinity of one another. The present results suggest that polymer-chain flexibility is essential for efficient energy migration among energy donors, leading to significant variation in the EET efficiency of donor/acceptor blends of varying flexible-coil donors. The maximum nonradiative energy-transfer efficiency of the —C7- and —C10-containing assemblies is a factor of 0.3 and 0.88 compared to that for the —C12-containing assembly. Thus, saturation of energy-transfer efficiency seems to be approached in going from 10- to 12-methylene flexible coil. This suggests that 12-methylene flexible coil segment may be the minimum length needed for sufficient polymer-chain flexibility for optimal energy transfer.

Interchromophore Distances in Supramolecular Assemblies

The measured Förster energy transfer efficiency can provide information about the average separation distances between donor and acceptor chromophores in the polymer nanocomposite assemblies.[1] The rate constant k_{DA} for Förster EET between energy donors (D) and acceptors (A) is given by :[1,18]
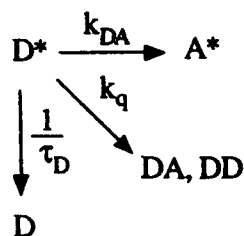
$$k_{DA} = \frac{1}{\tau_D} \left(\frac{R_{DA}}{r_{DA}}\right)^6 \qquad (3)$$

where r_{DA} is the average intersite distance between D and A chromophores, τ_D is the excited-state lifetime of the donor in the absence of the acceptor, and R_{DA} is the Förster radius. The related Förster EET efficiency χ is obtained as :[1,18]

$$\chi = \frac{k_{DA}}{\frac{1}{\tau_D} + k_{DA}} = \frac{1}{1 + \left(\frac{r_{DA}}{R_{DA}}\right)^6} \qquad (4)$$

The prediction of eqn.(4) is that the Förster energy transfer efficiency should be unity as donor

and acceptor chromophores are brought sufficiently close, i.e. as $(r_{DA}/R_{DA})^6$ approaches zero. This prediction is not observed in any of the three series of donor/acceptor assemblies investigated as the EET efficiency data in Figure 9 and Table 3 show. The reduced Förster efficiency suggests that an additional pathway for nonradiative excited state decay exists other than EET.[33] One possibility for this nonradiative and non-EET pathway is exciplex formation between the donor and acceptor chromophores; however, a detailed knowledge of this pathway is not essential to the subsequent analysis. The kinetic pathways for the deactivation of the excited donor are depicted below and the resulting nonradiative EET efficiency is given by :[33]

$$\chi = \frac{k_{DA}}{\frac{1}{\tau_D} + k_{DA} + k_q} = \frac{1}{1 + \frac{k_q}{k_{DA}} + \left(\frac{r_{DA}}{R_{DA}}\right)^6} \qquad (5)$$

where k_q is the rate constant for the nonradiative-decay pathway. From the measured asymptotic maximum nonradiative EET efficiency that corresponds to a negligibly small $(r_{DA}/R_{DA})^6$ value, the ratio of the nonradiative decay to the EET rate constant k_q/k_{DA} is determined. In the subsequent calculation of the interchromophore distance r_{DA}, the ratio k_q/k_{DA} is assumed to be a constant in the range of r_{DA} of interest, or equivalently that k_q has a similar distance dependence as k_{DA} (eqn.(3)). The validity of this assumption needs to be proved by more detailed studies in the future. Here, an estimate of the interchromophore distance was made using the known k_q/k_{DA} ratio and the experimental χ data, as described in eqn. (5).

The ratio k_q/k_{DA}, which measures the rate of nonradiative deactivation relative to the rate of nonradiative EET in the supramolecular donor/acceptor assemblies, varies from 5.9 in PPI/PI-C7 to 1.4 and 1.1 in PPI/PI-C10 and PPI/PI-C12, respectively (Table 2). The average intersite distance between donor and acceptor chromophores, r_{DA}, was in the range of 10—23, 11—23, and

16

12—25 Å in the PPI/PI-C7, PPI/PI-C10, and PPI/PI-C12 assemblies, respectively, depending on the acceptor concentration (Table 3). These interchromophore distances (r_{DA} values) are quite reasonable physical distances one might expect beween acceptor and donor chromophores in the present polymer nanocomposite assemblies. It is remarkable that the donor/acceptor interchromophore distances are similar in the three series of PBTVDA—PPI/PI-Cx assemblies. This suggests that r_{DA} is not the origin of the observed variation of nonradiative EET efficiency within the three series of donor/acceptor assemblies. The ratio k_q/k_{DA} appears to be the most significant factor that accounts for the observed EET efficiency variation with the donor rod-coil copolymer host. What this means is that the supramolecular structure of the light-absorbing donor host is very critical to the photophysical processes being balanced in the ratio k_q/k_{DA} which can be thought of as a measure of the "antenna power" of the energy donor component.

For comparison purposes, we have also estimated the average interchromophore distances among similar species in the assemblies, i.e. donor—donor (r_{DD}) and acceptor—acceptor (r_{AA}) intersite distances. These interchromophore distances were estimated by using a lattice gas model[34] : $r_{ii} = a_0/c^{1/3}$, where i= D or A, c is molecular concentration, and a_0 is a lattice constant (= $(3V/4\pi N_A)^{1/3}$, where V is the molar volume of polymer repeat unit which can be calculated from group-contribution formulation for molar volume of amorphous polymers,[35] and N_A is the Avogadro's number). The r_{DD} and r_{AA} values are 4—5 Å and 12—41 Å, respectively, depending on acceptor concentration (Table 3). Although the lattice gas model is a relatively crude approximation, the average intersite distances between the donor species and between the acceptor species are reasonable. This approach has been used to estimate intersite distances between dye molecules dispersed in amorphous polymer matrices.[34]

Conclusions

Highly efficient electronic energy transfer has been achieved in new polymer nanocomposite assemblies due to the optimal supramolecular structure of the energy donor copolymers that incorporate randomly distributed rigid-rod and flexible-coil segments. The critical

role of supramolecular structure in regulating energy-transfer efficiency was revealed by the observation that EET efficiency varied significantly with different nanocomposite donors consisting of 7-, 10-, and 12-methylene flexible coil. It was found that sufficient chain flexibility of the nanocomposite donor is essential to suppress the nonradiative deactivation pathways other than electronic energy transfer from donor to acceptor. By virtue of the thickness dependence of the energy-transfer efficiency, EET in these supramolecular assemblies was resolved into separate contributions of the nonradiative (Förster) and the radiative mechanisms. The nonradiative energy transfer efficiency increased with increasing acceptor concentration and saturated beyond a critical concentration which varied with the donor supramolecular structure. Spectroscopic ruler measurements, based on the nonradiative EET efficiency and Förster's equation, were performed to determine the interchromophore distances between the donors and acceptors in the assemblies, showing average intersite distances of 10—25 Å depending on the acceptor concentration. The present study has successfully explored the use of rod-coil copolymers and a π-conjugated rigid-rod polymer as components of efficient light-harvesting thin film assemblies while demonstrating the supramolecular structure regulation of singlet electronic energy transfer efficiency in the materials.

References

1. Guillet, J. E. *Polymer Photophysics and photochemistry*; Cambridge University Press : Cambridge, UK, **1985**.

2. Winnik, M. A., Ed. *Photophysical and Photochemical Tools in Polymer Science*; D. Reidel Publishing Co. : Dordrecht, The Netherlands, **1986**.

3. Webber, S. E. *Chem. Rev.* **1990**, 90, 1469-1482.

4. Fox, M. A.; Jones Jr., W. E.; Watkins, D. M. *Chem. Engr. News* **1993**, Mar. 15, 38-48.

5. Fox, M. A.; Chanon, M., Eds. *Photoinduced Electron Transfer*, Elsevier : Amsterdam, **1989**.

6. Fox, R. B.; Cozzens, R. F. *Macromolecules* **1969**, 2, 181-184.

7. Fox, R. B.; Price, T. R.; Cozzens, R. F.; McDonald, T. R. *J. Chem. Phys.* **1972**, 57, 534-541.

8. Holden, D. A.; Guillet, J. E. *Macromolecules* **1980**, 13, 289-295.

9. Aspler, J. S.; Hoyle, C. E.; Guillet, J. E. *Macromolecules* **1978**, 11, 925-929.

10. Guillet, J. E.; Rendall, W. A. *Macromolecules* **1986**, 19, 224-230.

11. Strurtevant, J. L.; Webber, S. E. *Macromolecules* **1989**, 22, 3564-3571.

12. Bai, F.; Chang, C.-H.; Webber, S. E. *Macromolecules* **1986**, 19, 2484-2489.

13. Byers, J. D.; Parsons, W. S.; Friesner, R. A.; Webber, S. E. *Macromolecules* **1990**, 23, 4835-4844.

14. Nowakowska, M.; White, B.; Vogt, S.; Guillet, J. E. *J. Polym. Sci. : Polym. Chem.* **1992**, 30, 271-277.

15. Nowakowska, M.; Guillet, J. E. *Macromolecules* **1991**, 24, 474-478.

16. White, B.; Nowakowska, M.; Vancso, G. J.; Guillet, J. E. *Macromolecules* **1991**, 24, 2903-2906.

17. Johnson, G. E. *Macromolecules* **1980**, 13, 145-152.

18. Förster, T. in *Modern Quantum Chemistry : Istanbul Lectures*; Sinanoglu, O., Ed.; Academic Press : New York, **1965**, pp. 93-137.

19. Styrer, L. *Ann. Rev. Biochem.* **1978**, 47, 819-846.

20. Liu, G.; Guillet, J. E.; Vlegels, M.; Goethals, E. J. *Macromolecules* **1991**, 24, 4094-4100.

21. Duhamel, J.; Yekta, A.; Ni, S.; Khaykin, Y.; Winnik, M. A. *Macromolecules* **1993**, 26, 6255-6260.

22. Morawetz, H. *Science* **1988**, 240, 172-176.

23. Major, M. D.; Torkelson, J. M.; Brearley, A. M. *Macromolecules* **1990**, 23, 1700-1710.

24. Guillet, J. E.; Hoyle, C. E.; Maccallum, J. R. *Chem. Phys. Lett.* **1978**, 54, 337-341.

25. Mahrt, R.; Yang, J.-P.; Greiner, A.; Bässler, H.; Bradley, D. D. C. *Makromol. Chem.*

Rapid Commun. **1990**, 11, 415-421.

26. (a) Osaheni, J. A.; Jenekhe, S. A. Submitted for publication; (b) Jenekhe, S. A.; Osaheni, J. A. *Nature*, Submitted.

27. Agrawal, A. K.; Jenekhe, S. A. *Macromolecules* **1993**, 26, 895-905.

28. Yang, C. J.; Jenekhe, S. A. *Chem. Mater.* **1991**, 3, 878-887.

29. Schaefer, D. W.; Mark, J. E., Eds. *Polymer Based Molecular Composites*; Materials Research Society Proceedings; Materials Research Society : Pittsburgh, **1990**; Vol. 171.

30. (a) Roberts, M. F.; Jenekhe, S. A. *Chem. Mater.* **1994**, 6, 135-145.
    (b) Vanherzeele, H. Meth, J. S.; Jenekhe, S. A.; Roberts, M. F. *Appl. Phys. Lett.* **1991**, 58, 663-665.

31. Guilbault, G. G., Ed. *Practical Fluorescence*, 2nd ed.; Marcel Dekker Inc. : New York, **1990**.

32. Berlman, I. B. *Energy Transfer Parameters of Aromatic Compounds*; Academic Press : New York, **1973**.

33. Lakowicz, J. R. *Principles of Fluorescence Spectroscopy*; Plenum Press : New York, **1983**, pp. 303-336.

34. Borsenberger, P. M. *J. Appl. Phys.* **1992**, 72, 5283-5287.

35. Van Krevelen, D. W. *Properties of Polymers : Their Estimation And Correlation with Chemical Structure*, Elsevier : Amsterdam, **1976**.

Table 1. Optical absorption edge E_g, absorption and the emission maxima, and fluorescence quantum efficiency ϕ of EET chromophores

chromophore	E_g (eV)	absorption λ_{max} (nm)	emission λ_{max} (nm)	ϕ (%)
PPI/PI-C7	2.61	370	530, 560	0.31
PPI/PI-C10	2.61	370	530, 560	0.64
PPI/PI-C12	2.61	370	530, 560	0.74
PBTVDA	2.00	530	650	0.58

Table 2. Förster radii for singlet electronic energy transfer from host donors to PBTVDA acceptor

host donor	R_{DA} (Å)	R_{DD} (Å)	R_{AA} (Å)	k_q/k_{DA}
PPI/PI-C7	19.1	9.0	16.3	5.9
PPI/PI-C10	21.0	10.0	16.3	1.4
PPI/PI-C12	22.5	11.7	16.3	1.1

Table 3. Förster energy-transfer efficiency and interchromophore distances in the polymer nanocomposite assemblies

host donor	mol % PBTVDA	χ (%)	r_{DA} (Å)	r_{DD} (Å)	r_{AA} (Å)
PPI/PI-C7	0.4	10.1	23.0	4.2	33.3
	0.9	13.2	17.8	4.2	26.5
	1.3	13.9	15.3	4.2	23.1
	2.4	14.2	12.5	4.3	18.9
	3.4	14.2	12.5	4.3	16.7
	5.4	14.3	10.8	4.3	14.4
	7.2	14.4	9.8	4.3	13.0
PPI/PI-C10	0.2	24.5	23.0	4.5	41.1
	0.6	28.7	21.4	4.5	30.0
	1.0	30.8	20.6	4.5	25.5
	1.5	36.7	17.6	4.5	21.9
	2.5	38.6	16.2	4.5	18.6
	3.4	40.9	13.3	4.5	16.7
	3.6	39.6	15.3	4.5	16.4
	5.5	40.9	13.3	4.6	14.2
	7.3	41.7	10.9	4.6	13.0
PPI/PI-C12	0.3	26.0	24.7	4.6	39.4
	0.6	29.6	23.5	4.6	30.2
	1.2	36.0	21.2	4.7	23.9
	1.6	37.6	20.5	4.7	21.3
	2.4	45.5	15.7	4.7	18.9
	2.9	45.8	15.3	4.7	17.7
	4.2	46.5	14.4	4.7	15.6
	4.9	46.8	13.9	4.7	14.9
	6.5	47.3	12.6	4.7	13.5
	8.7	47.6	11.6	4.8	12.2

Figure Captions

Figure 1. ^{1}H NMR spectrum of PPI/PI-C7 in $GaCl_3/CD_3NO_2$.

Figure 2.   DSC thermograms of PPI/PI-C12 (a), PBTVDA (b), and the 8.7-mol% blend of PBTVDA with PPI/PI-C12 (first heating (c), second heating (d)) at a heating rate of 20 °C/min.

Figure 3.   Optical absorption spectra of PPI/PI-C12 (a) and PBTVDA (b), and fluorescence spectra of PPI/PI-C12 (c) and PBTVDA (d).

Figure 4.   Fluorescence spectra of PPI/PI-C7 (a), PPI/PI-C10 (b), PPI/PI-C12 (c), and PBTVDA (d).

Figure 5.   Fluorescence spectra of the 3.4-mol% blend of PBTVDA with PPI/PI-C12 when excited at 420 nm (a) and 530 nm (b).

Figure 6.   Acceptor concentration (mol % PBTVDA) dependence of thin films of PPI/PI-C12 donor/acceptor assemblies : 1.2 mol% (a), 2.4 mol% (b), 2.9 mol% (c), 4.2 mol% (d), 4.9 mol% (e), and 6.5 mol% (f).

Figure 7.   Film thickness dependence of the emission of the blend of 2.9 mol% PBTVDA with PPI/PI-C12 : 29 nm (a), 38 nm (b), 57 nm (c), 68 nm (d), and 96 nm (e) film.

Figure 8.   Film thickness dependent efficiency $\chi(d)$ for electronic energy transfer of 2.9 mol % PBTVDA (a) and 0.6 mol% PBTVDA (b) in PPI/PI-C12.

Figure 9.   Acceptor concentration (mol% PBTVDA) dependence of the total energy-transfer efficiency (open symbol) and the Förster energy-transfer efficiency (filled symbol) in the donor/acceptor nanocomposite assemblies : PPI/PI-C7 (a); PPI/PI-C10 (b); and PPI/PI-C12 (c).

Chart 1
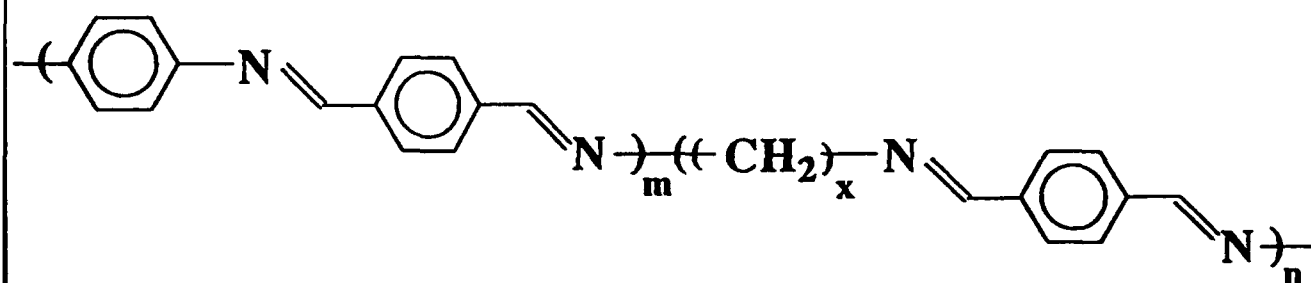
x = 7, 10, 12
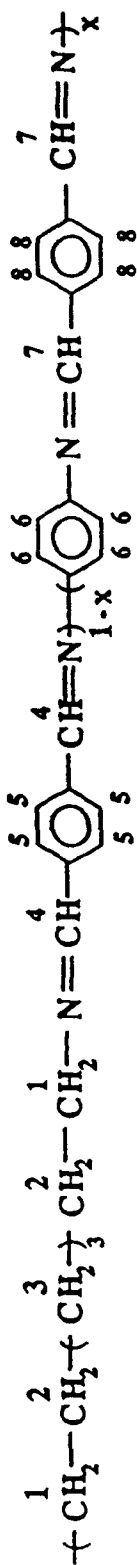
PPI/PI-Cx

PBTVDA
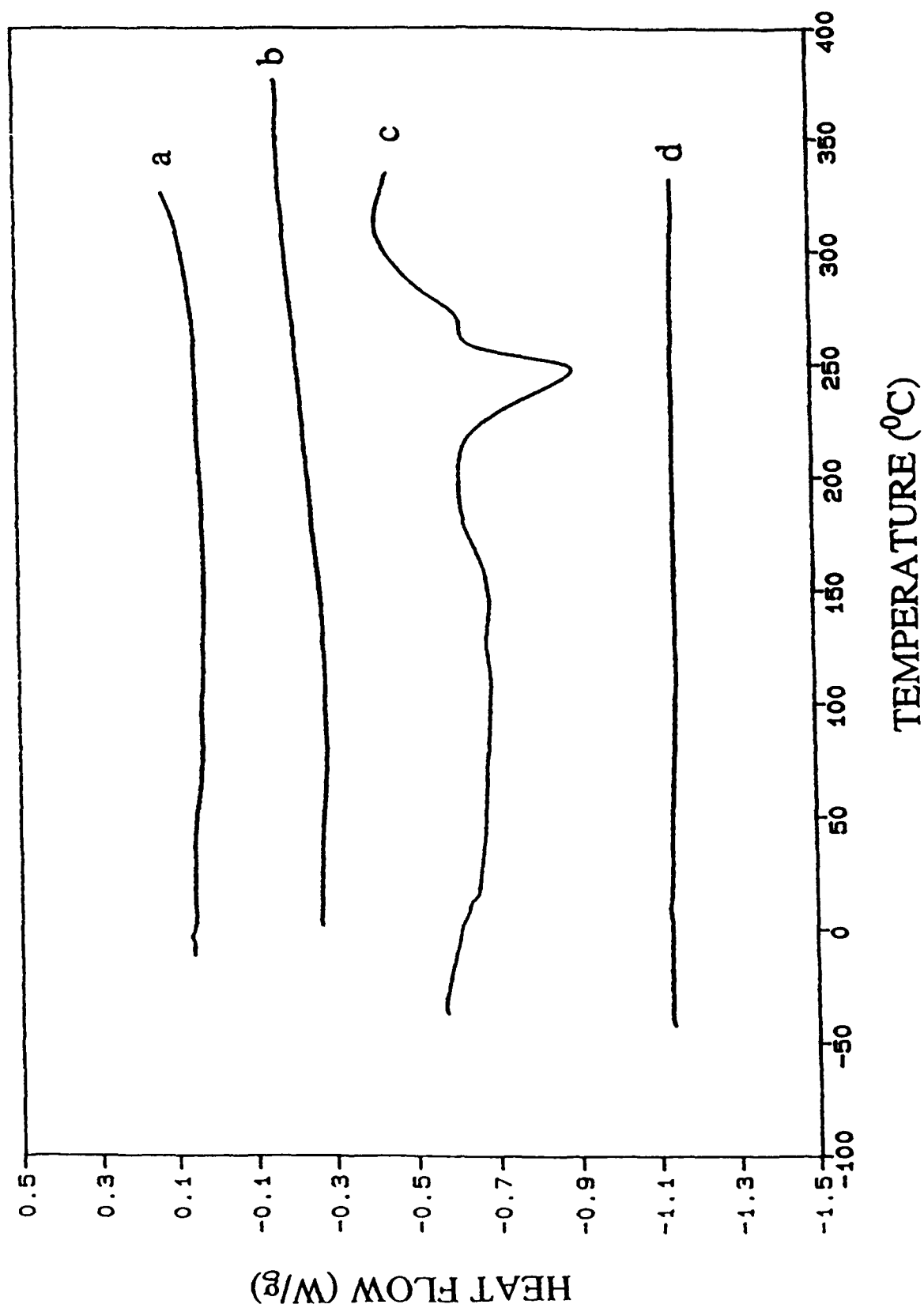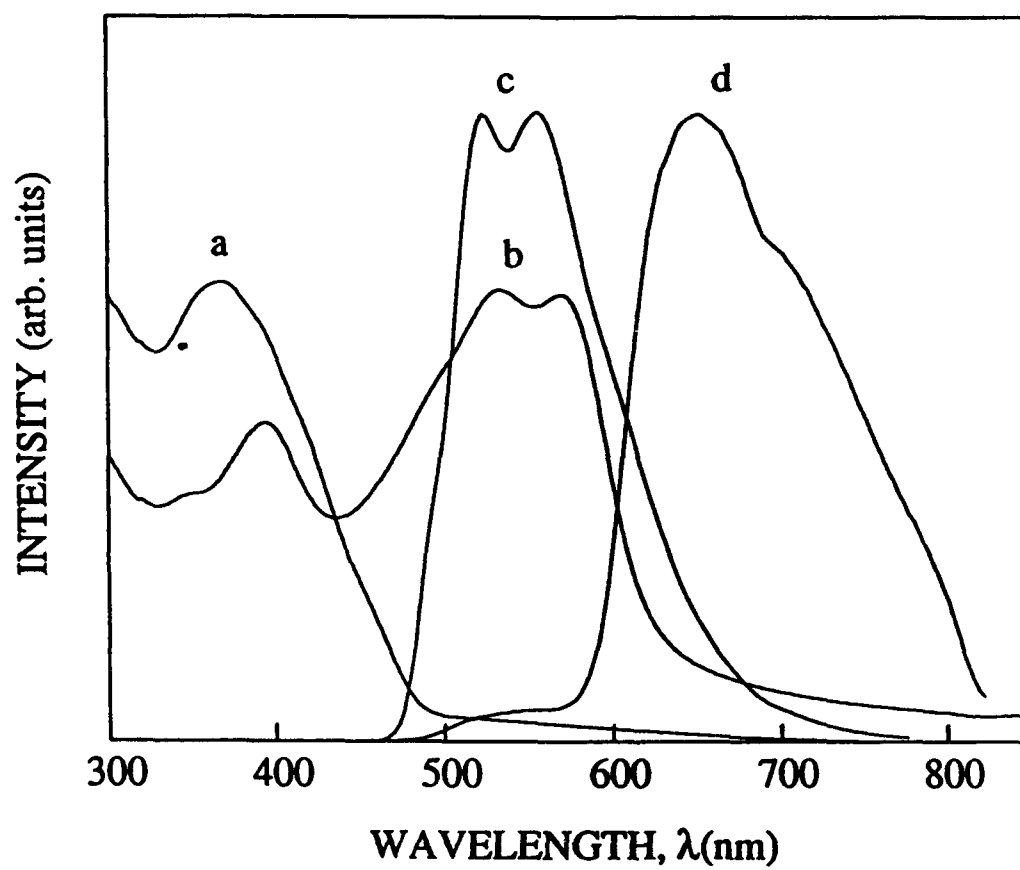
Chart 2

+

Acceptor
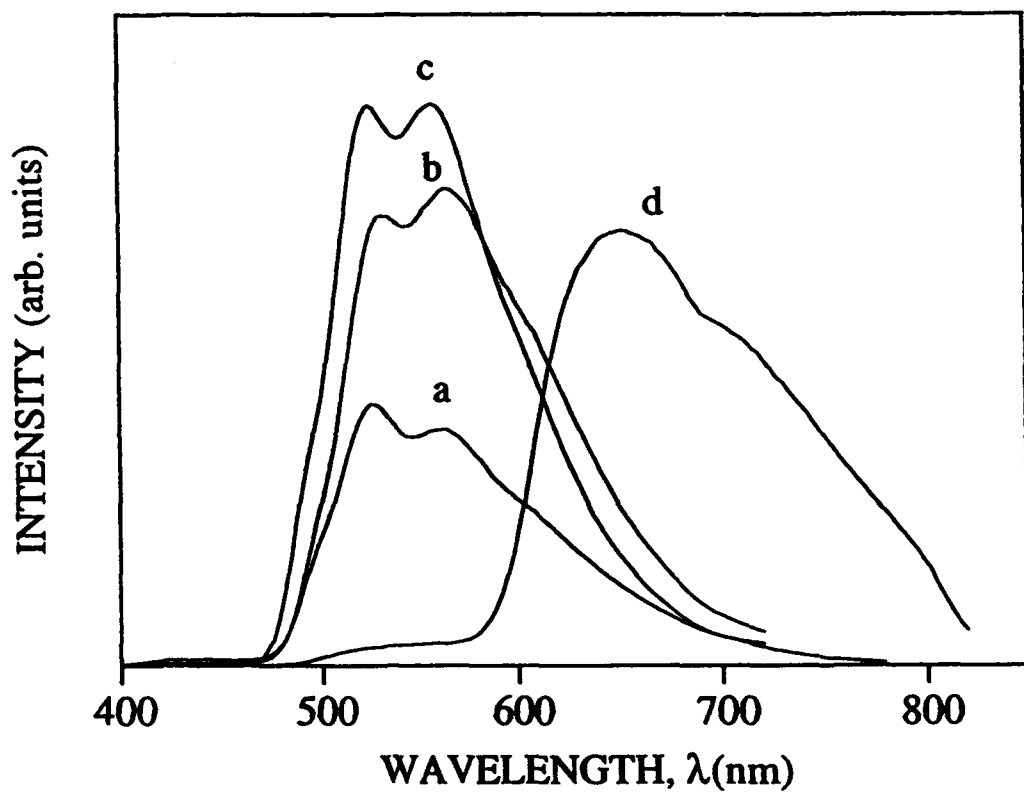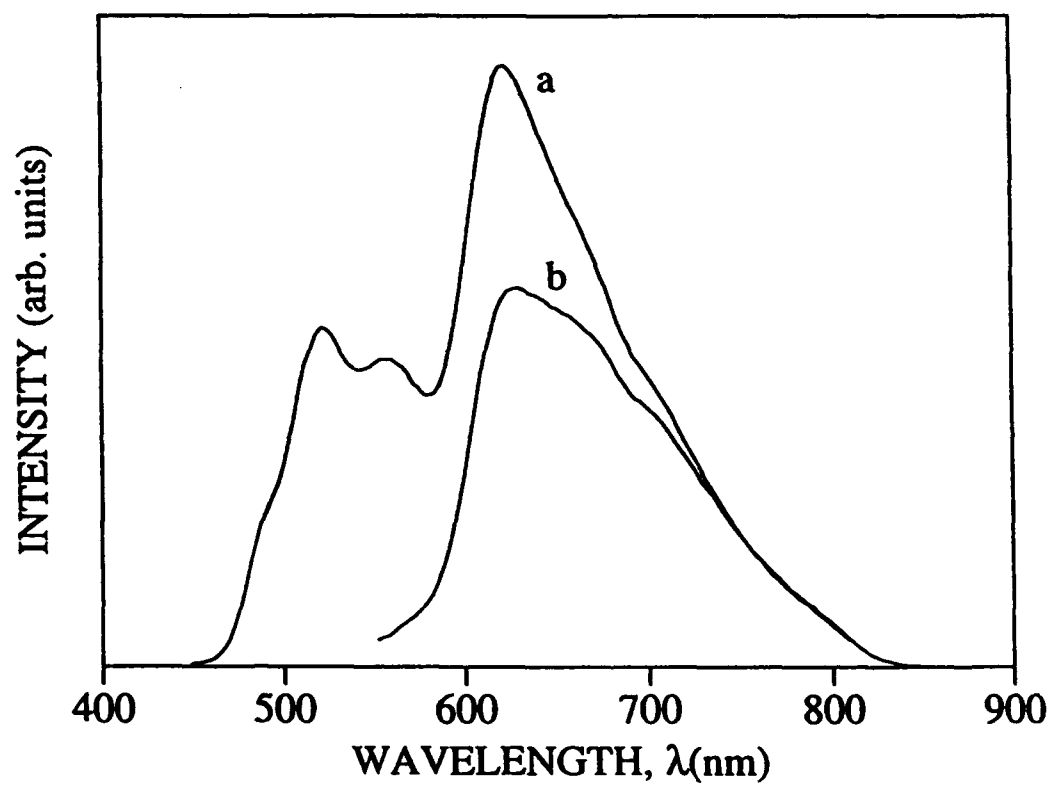
Donor

Chart 3

Energy Migration

Energy Transfer

Fig. 1
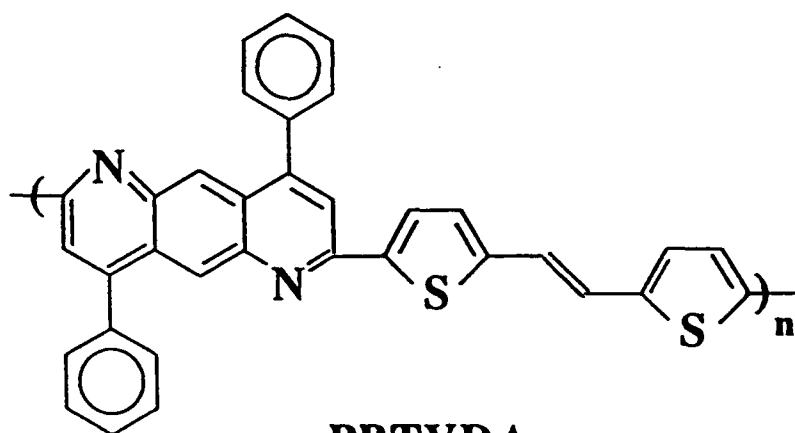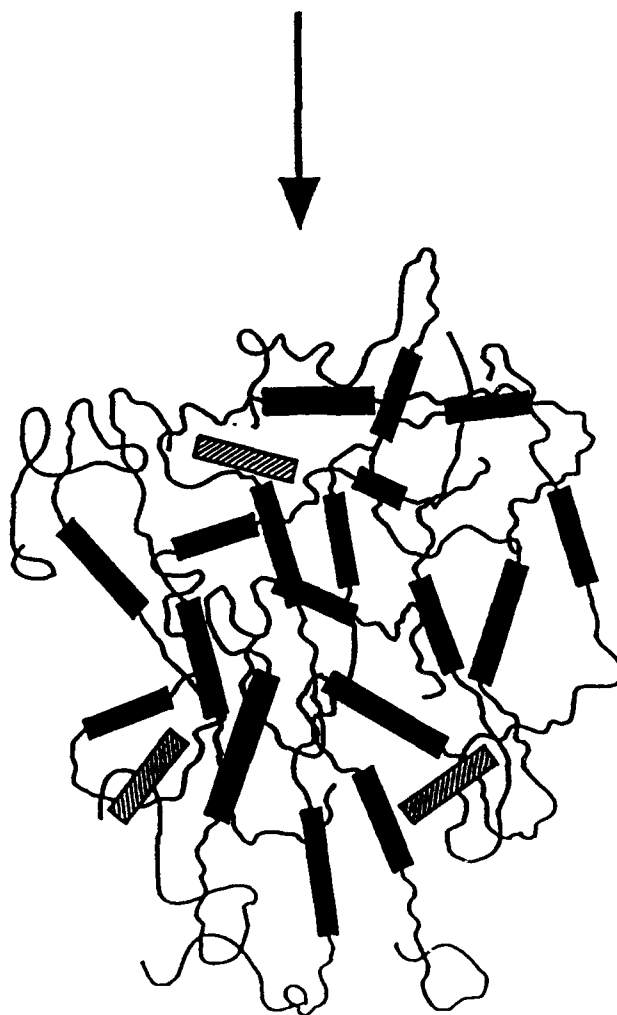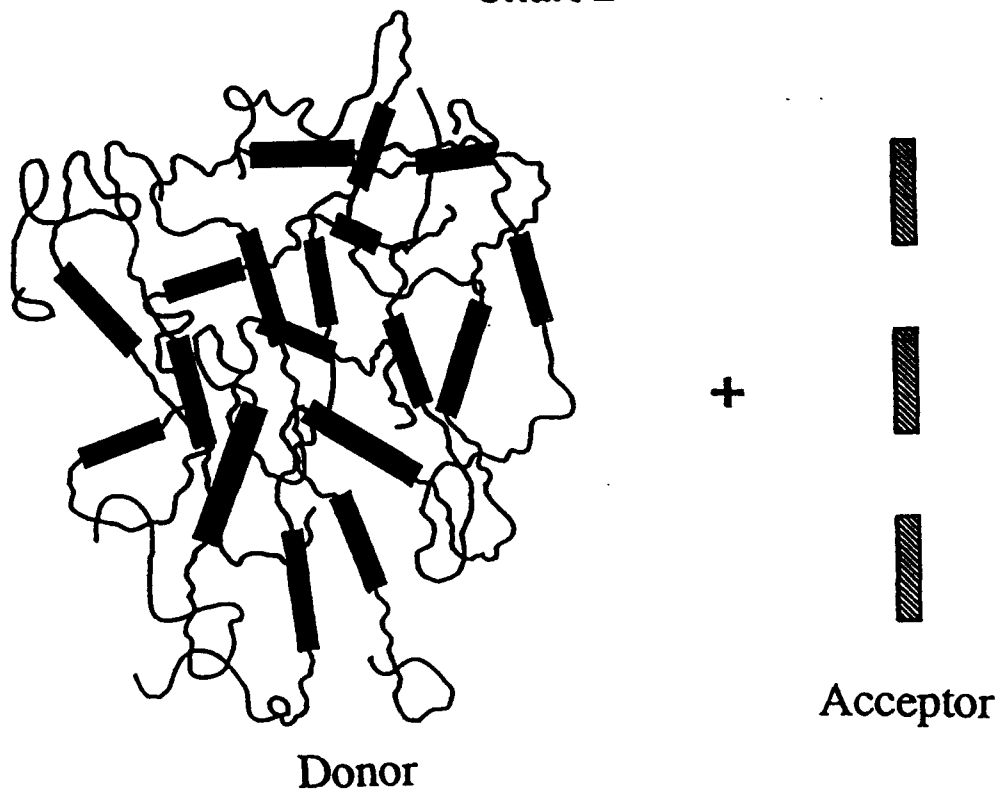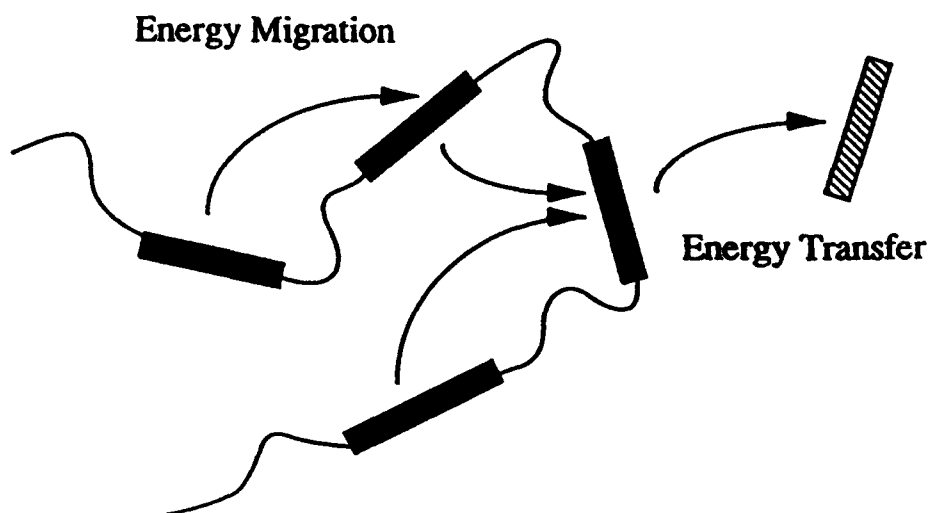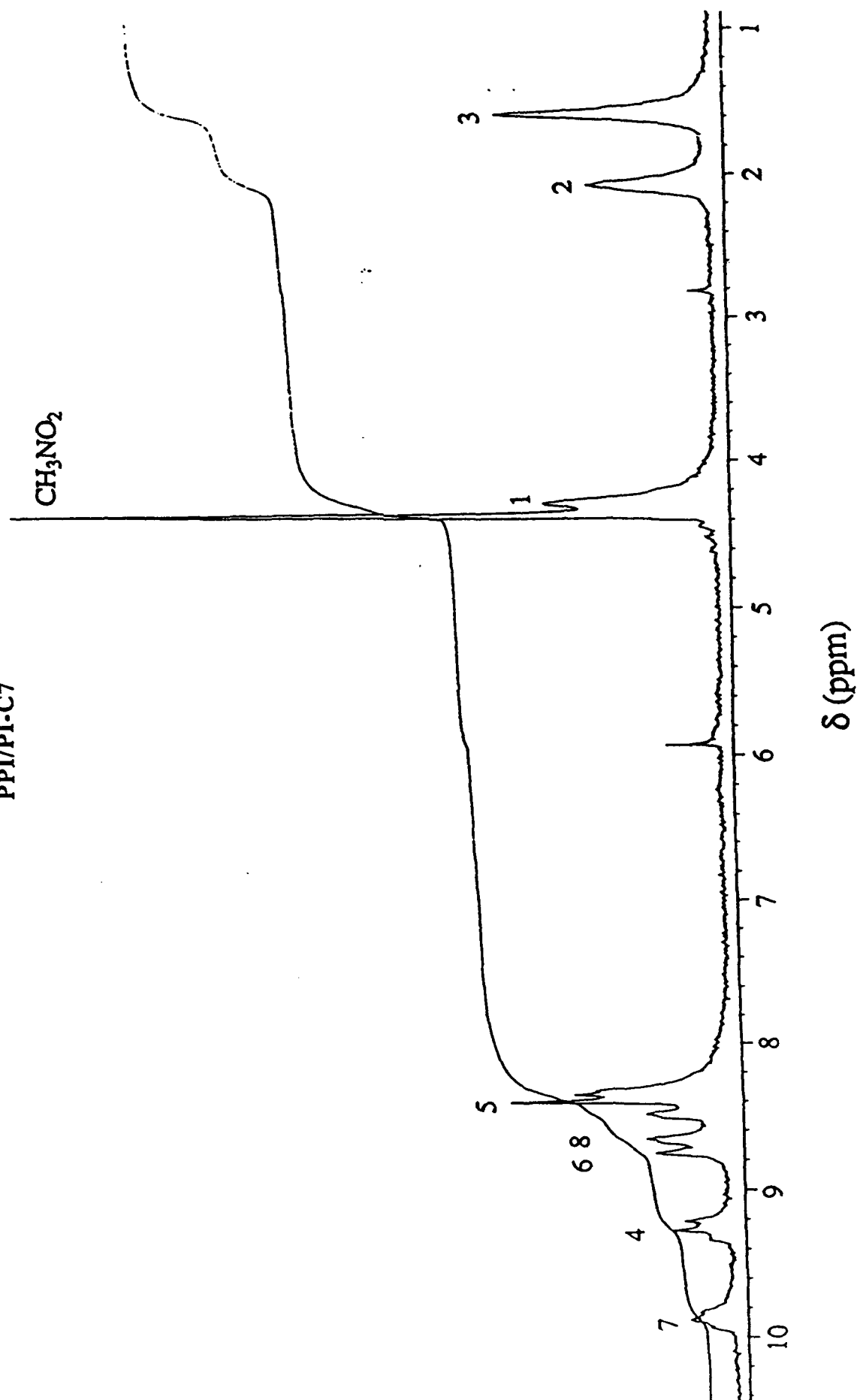
Fig. 2

Fig 3

Fig. 4

Fig. 5

Fig. 6

Fig. 7

Fig. 8

Fig. 9